Simplified model for a rivulet spreading down an inclined wetted plate

Martin Isoz

Institute of Chemical Technology, Prague

Keywords: rivulet, fluid dynamics, liquid spreading

Abstract

Rivulet type flow down an inclined plate is of great importance in many engineering areas including packed columns design and catalytic reactors modeling. Combining a simplified solution of the Navier-Stokes equation for a rectilinear rivulet and the Cox-Voinov law for an axisymmetric spreading of a perfectly wetting liquid, we derived a semi-analytical model of the liquid flow in a spreading rivulet. The proposed model was used to characterize the flow of a liquid in dependence of the plate inclination angle, rivulet dynamic contact angle and liquid flow rate. The presented modeling method provides an insight on the liquid flow properties without the necessity of numerically solving the corresponding PDEs.

1 Introduction

Flow characteristics of a gravity driven, spreading trickle of a liquid, is of the key importance throughout many areas of chemical engineering, including the ones concerning the mass transfer [1], trickle bed reactors [2], heat exchangers [3] and various coating processes [4].

Eventhough the rivulet type flow can be modeled using various CFD methods [1,5], such methods are still too complex to be used in the engineering practice and too computationally demanding for the parametric studies of the rivulet behavior.

A simplified solution to the problem of the rivulet type flow has been studied since 1960's. The pioneering studies by Towell and Rothfeld [6], Allen and Biggin [7], Bentwich et al. [8] and Fedotkin et al. [9] have led to a substantial amount of subsequent work on rectilinear rivulet flow. For example, Benilov [10] performed a stability analysis for the rivulet flow down

an inclined substrate and Duffy and Moffat [11] used the solution available for the rectilinear rivulet flow to describe the flow with prescribed volume flux and non-zero contact angle over a cylinder of large radius. For further informations on the topic of unidirectional (rectilinear) rivulet flow, see [12–15] and many references therein.

The problem of the physics of the contact line region of a rivulet was first taken into account by Davis [16] and revisited from another point of view by Shetty and Cerro [17]. However, a literature covering the topic of modeling the flow of a spreading rivulet is still limited to various CFD methods (e.g. [1,18,19]) or the spreading rivulet stability analysis (see [20] and references therein).

A rather different approach from the previous studies was taken in the presented work. We used the solution for the unidirectional flow of a slender and shallow rivulet with prescribed volume flux and non-zero contact angle to describe the locally unidirectional flow of a rivulet with slowly varying both contact angle and width. To link the change in contact angle with development of the rivulet width, we applied the Cox-Voinov law [21,22] for the axisymmetric spreading of a perfectly wetting liquid on a horizontal substrate in time coupled with an approximative transformation from time to a spatial coordinate.

A method for simulation of the flow in a spreading rivulet was derived for the case of a wetted plate inclined by an angle $\alpha \in (0; \pi)$ to the horizontal.

The studied problematics can be divided in two main parts: the specification of the rivulet gas-liquid (GL) interface shape and the calculation of the velocity field in it. Furthermore, it is convenient to analyze separately the case of a rivulet flowing on an inclined plate ($\alpha < \pi/2$), underneath it ($\alpha > \pi/2$) and the special case of a vertical plate ($\alpha = \pi/2$).

For the flow on a vertical plate or for a very shallow rivulet in which the gravity can be neglected, the problem of finding the shape of GL interface of the rivulet was reduced from the solution of the corresponding system of the Navier-Stokes equations to the repeated solution of one non-linear algebraic equation. The other cases have to be treated numerically. However, the proposed algorithms are all based on a solution of a single ordinary differential equation.

The velocity field in the spreading rivulet was obtained on a purely numerical basis. We used a technique based on a principle of particle image velocimetry (PIV), thoroughly described in a review [24], but with followed "particles" created numerically.

2 Coordinate system and simplifying assumptions

The case of a steady flow of a thin symmetric rivulet down an inclined wetted plate was studied in the Cartesian coordinate system $Oxyz$ with the x axis down the line of the greatest slope, the y axis horizontal and the z axis normal to the substrate $z = 0$. The used coordinate system as well as the most important symbols are depicted in the Fig. 1.

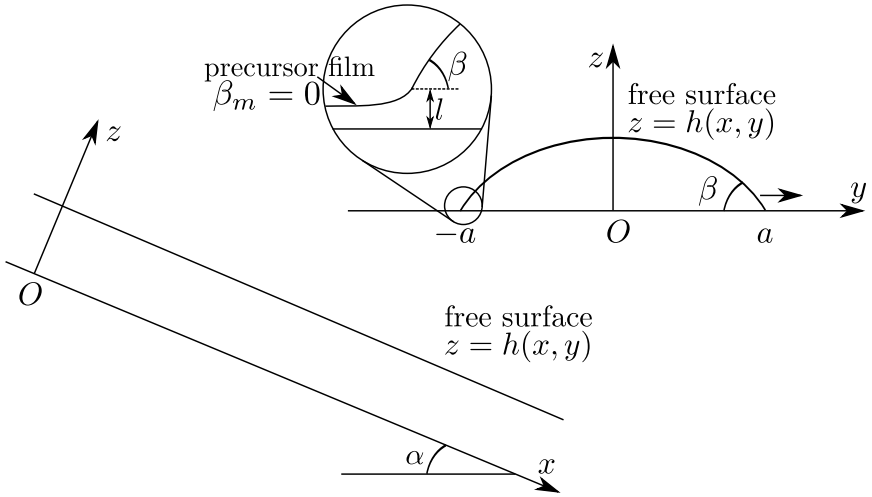

Figure 1: Used coordinate system with the basics of rivulet spreading notation. α is the plate inclination angle, β and β_m are the apparent (dynamic) and the microscopic contact angles, a is the rivulet half width.

The proposed method for modeling of a gravity driven spreading rivulet flowing down an inclined wetted plate was derived under the following simplifications,

1. The studied liquid is Newtonian, ρ, μ and γ are constant.
2. The rivulet profile shape is constant in time. Furthermore, Q is constant not only in time, but also in all spatial directions.
3. There is no shear between the gas and liquid phases.
4. The liquid velocities in the directions transversal and normal to the plate are negligible in comparison to the one in its longitudinal direction, $u \gg v \sim w$. The inertial effects can be neglected in y and z directions.

5. The gravity is the only acting body force.

6. The rivulet is shallow. Its dynamic contact angles are assumed small, $\beta(x) \ll 1$, and its GL interface is nearly flat, $h_y(x,y) \ll 1$.

7. There is a thin precursor film of height l on the whole studied surface. Thus there is no contact angle hysteresis and $\beta_m = 0$. The height of the precursor film, l, can also be taken as the intermediate region length scale well separating the inner and outer solution for the profile shape [23].

3 Specification of the GL interface shape

With the above listed simplifying assumptions, the parallel between the spreading of a rivulet along an inclined plate and the spreading of a static objects in time can be found.

At first, the system of Navier-Stokes equations for an unidirectional flow, as presented by Duffy and Moffatt [11], is solved to obtain a local description of a spreading rivulet. Then, the Cox-Voinov law is used to describe the evolution of the boundary conditions, and thus the rivulet gas-liquid (GL) interface shape, along the plate.

3.1 Static rivulet

For the case of a rectilinear steady flow of a shallow rivulet, the Navier-Stokes equations can be simplified via 'thin-film theory' to,

$$\begin{aligned} 0 &= -p_x + \rho g \sin\alpha + \mu u_{zz} \\ 0 &= -p_y \\ 0 &= -p_z - \rho g \cos\alpha \end{aligned} \tag{1}$$

and integrated subject to the boundary conditions,

$$\begin{aligned} z &= 0: && u = u(y,z) = 0 \\ z &= h: && p = p_A - \gamma h_{yy} \quad \text{and} \quad u_z = 0 \\ y &= \pm a: && h = 0 \quad \text{and} \quad h_y = \pm \tan\beta. \end{aligned} \tag{2}$$

Solution of the system (1) with boundary conditions (2) yields the following equation describing the shape the GL interface of an uniform rivulet

for the three cases of different plate inclination angles, $\alpha < \pi/2$, $\alpha = \pi/2$ and $\alpha > \pi/2$ indicated as (i), (ii) and (iii), respectively.

$$h(\zeta) = \begin{cases} \dfrac{a\tan\beta}{\sqrt{\mathrm{B}}}\left(\dfrac{\cosh\sqrt{\mathrm{B}} - \cosh\sqrt{\mathrm{B}}\zeta}{\sinh\sqrt{\mathrm{B}}}\right) & (i) \\ \dfrac{a\tan\beta}{2}(1-\zeta^2) & (ii) \\ \dfrac{a\tan\beta}{\sqrt{\mathrm{B}}}\left(\dfrac{\cos\sqrt{\mathrm{B}}\zeta - \cos\sqrt{\mathrm{B}}}{\sin\sqrt{\mathrm{B}}}\right) & (iii) \end{cases}, \tag{3}$$

where B is the Bond number of the problem, defined as $\mathrm{B} = a^2\rho g|\cos\alpha|/\gamma$, representing the ratio of volume and surface forces in the rivulet and ζ is the y coordinate non-dimensionalized by the rivulet half-width, $\zeta = y/a$.

In addition, a multiplication factor useful for non-dimensionalization of the rivulet height arises from the case (ii) in the equation (3),

$$\tilde{h}(\zeta) = \frac{2h(\zeta)}{a\tan\beta} \tag{4}$$

Case (iii) of the solution (3) has a singularity at $\mathrm{B} = \pi^2$ and thus is only sensible if B is restricted by $0 \leq \mathrm{B} \leq \pi^2$. The singularity corresponds to the dripping of the liquid from the plate which occurs at high B, when the surface tension forces are not strong enough to keep the rivulet in contact with the plate. The effects of changes in the Bond number on the GL interface shape are depicted in the Fig. 2.

With the liquid volumetric flux taken as a fixed parameter, the rivulet half width, a, and its apparent contact angle, β, are bonded with the relation,

$$\frac{Q}{a} = \int_{-1}^{1}\int_{0}^{h(\zeta)} u(\zeta, z)\,\mathrm{d}z\,\mathrm{d}\zeta = \int_{-1}^{1}\int_{0}^{h(\zeta)} \frac{\rho g\sin\alpha}{2\mu}\left(2h(\zeta)z - z^2\right)\,\mathrm{d}z\,\mathrm{d}\zeta. \tag{5}$$

After the integration, one obtains the following equation for the rivulet contact angle and half width,

$$\frac{\mu Q}{a^4\rho g\sin\alpha\tan^3\beta} = F(\mathrm{B}) \tag{6}$$

and

$$F(\mathrm{B}) = \begin{cases} \dfrac{54\sqrt{\mathrm{B}}\cosh\sqrt{\mathrm{B}} + 6\sqrt{\mathrm{B}}\cosh 3\sqrt{\mathrm{B}} - 27\sinh\sqrt{\mathrm{B}} - 11\sinh 3\sqrt{\mathrm{B}}}{36\mathrm{B}^2\sinh^3\sqrt{\mathrm{B}}} & (i) \\ \dfrac{4}{105} & (ii) \\ \dfrac{27\sin\sqrt{\mathrm{B}} + 11\sin 3\sqrt{\mathrm{B}} - 54\sqrt{\mathrm{B}}\cos\sqrt{\mathrm{B}} - 6\sqrt{\mathrm{B}}\cos 3\sqrt{\mathrm{B}}}{36\mathrm{B}^2\sin^3\sqrt{\mathrm{B}}} & (iii) \end{cases} \tag{7}$$

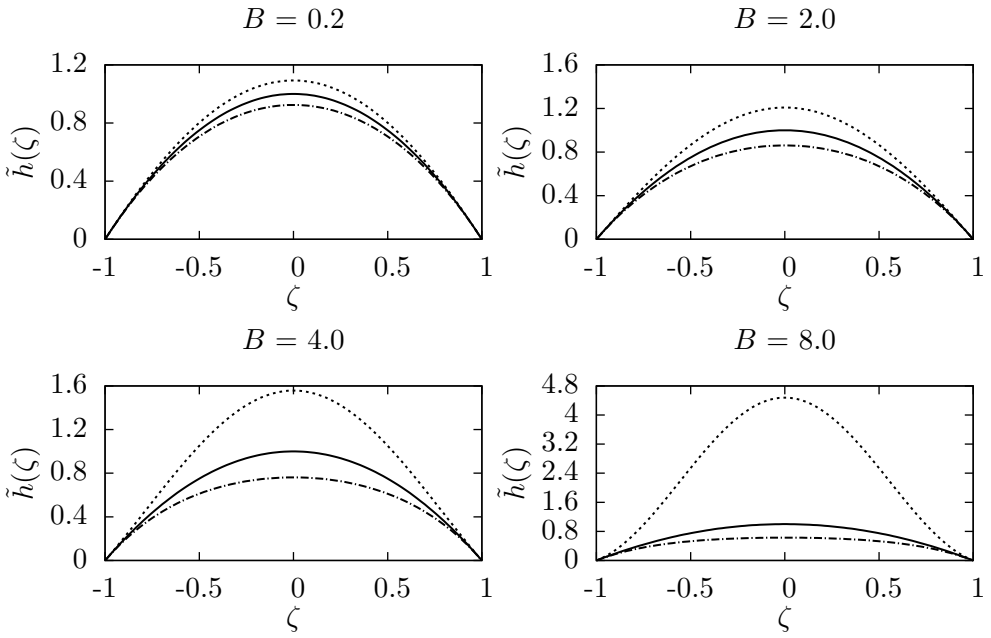

Figure 2: Scheme of the effects of changes in the Bond number on the rivulet GL intarface shape. In the case (i) (-·-·-), the interface is flattened as the gravity effects grows stronger in comparison with the surface tension. In the case (iii) (·····) the increase of B has the narrowing effect on the rivulet GL interface. Case (ii) (——) is depicted for reference. Rivulet contact angle and semi-width are fixed at $\beta = 0.05$ and $a = 0.01\,\mathrm{m}$.

Again, the liquid volumetric flow rate can be non-dimensionalized using the expression for the flow rate on a vertical plate,

$$\tilde{Q} = \frac{105\mu}{4a^4\rho g \sin\alpha \tan^3\beta} Q = \frac{105\rho g \mu \cos^2\alpha}{4\gamma^2 \sin\alpha \tan^3\beta} \frac{Q}{\mathrm{B}^2}. \tag{8}$$

The dependence of the liquid dimensionless flow rate, $\tilde{Q}$, on the plate inclination angle, α, is shown in the Fig. 3 (a) and the dependece of $\tilde{Q}$ on the rivulet Bond number, B, in the Fig. 3 (b).

In the Fig. 3 (b), a different asymptotic behavior of the solution can be observed for the cases of a rivulet flowing on, (i), and under, (iii), an inclined plate,

$$\begin{aligned} (i): &\quad \lim_{\mathrm{B}\to\infty} \tilde{Q}(\mathrm{B}) = 0 \\ (iii): &\quad \lim_{\mathrm{B}\to\pi^2_-} \tilde{Q}(\mathrm{B}) = \infty \end{aligned} \tag{9}$$

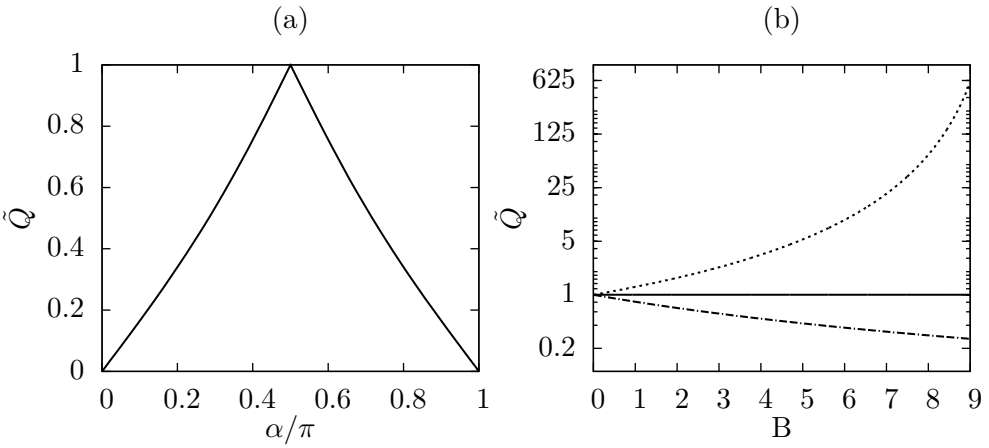

Figure 3: Dependence of the dimensionless flow rate, $\tilde{Q}$, on the plate inclination angle, (a), and on the Bond number, (b). In the Figure on the right side are distinguished the three different cases, (i) for $\alpha < \pi/2$ (-·-·-), (ii) for $\alpha = \pi/2$ (——) and (iii) for $\alpha > \pi/2$ (·····).

Moreover, for rivulet flowing down a vertical plate or for a rivulet with neglectable effects of the gravity on its GL interface shape, the equation (6) can be solved analytically to obtain the following explicit relation between a and β,

$$a = \eta \frac{1}{\tan^{3/4}\beta}, \quad \eta = \left(\frac{4\mu Q}{105\rho g \sin\alpha}\right)^{\frac{1}{4}}. \tag{10}$$

For the other cases, the equation (6) has to be solved numerically.

3.2 Spreading rivulet

In the previous section, the GL interface shape of a rectilinear steady rivulet was studied. In this section, the obtained results are used to locally describe the GL interface shape of a spreading rivulet. The local descriptions are bounded together by the Cox-Voinov law to obtain an approximate shape of the GL interface of a spreading rivulet.

The difference between a static, uniform, rivulet and the spreading one is in the formulation of the boundary conditions (2). For a static rivulet, β and a are constant all along the rivulet but for a spreading rivulet, these two become functions of the problem longitudinal coordinate, x.

Hence, for being able to profit from the solution for an uniform rivulet, it is necessary to provide a relation for the evolution of $\beta(x)$ and $a(x)$ along the rivulet.

In the review [23], the Cox-Voinov law for the case of a symmetric 2D object spreading on a horizontal substrate was derived in the form,

$$\beta(t)^3 = 9\frac{\mathrm{d}a(t)}{\mathrm{d}t}\frac{\mu}{\gamma}\ln\left(\frac{a(t)}{2e^2 l}\right), \tag{11}$$

with $a(t)$ being the object characteristic dimension. For the case of a narrow axially symmetric stripe of a liquid, $a(t)$ represents its half width.

The resulting equation is a first order ordinary differential equation for two unknown functions, $\beta(t)$ and $a(t)$ and one free parameter, l, corresponding to the intermediate region length scale (see Fig. 1 and [21–23]).

In the case of a steady rivulet of a liquid flowing and spreading down an inclined wetted plate, the time coordinate in (11) can be transformed in the spatial coordinate, x.

Neglectable effects of the gravity The main thought of the modeling of a spreading rivulet GL interface is described using the simplest case of a vertical plate, or neglectable effects of gravity on the GL interface shape. With an assumption of a small contact angles all along the rivulet, $\beta(x) \ll 1$, $\forall x \in \langle 0; L\rangle$, the equation (10) can be simplified to

$$a \doteq \eta\frac{1}{\beta^{3/4}}. \tag{12}$$

Substituting for a from (12) to (11), one arrives at

$$\beta^{19/4} = -A\frac{\mathrm{d}\beta}{\mathrm{d}t}\ln\left(\frac{B}{\beta^{3/4}}\right), \qquad \beta = \beta(t), \quad A = \frac{27}{4}\frac{\eta\mu}{\gamma}, \quad B = \frac{\eta}{2e^2 l}. \tag{13}$$

Solution of (13) yields an implicit relation for $\beta(t)$,

$$t - \frac{4}{15}\frac{A}{\beta^{15/4}}\left[\ln\left(\frac{B}{\beta^{3/4}}\right) - \frac{1}{5}\right] + C = 0. \tag{14}$$

The integration constant, C, is specified by the initial condition, $\beta(0) = \beta_0$,

$$C = \frac{4}{15}\frac{A}{\beta_0^{15/4}}\left[\ln\left(\frac{B}{\beta_0^{3/4}}\right) - \frac{1}{5}\right]. \tag{15}$$

Now, let us take the three phase point of one transversal cut through the rivulet and denote it as τ. The equation (14) describes the movement of τ in the direction of the y axis in time and the effects of this movement on the shape of the 2D GL interface of the chosen transversal cut.

For the description of the rivulet interface shape along the plate, the relation between the movement of τ in time and the movement of the chosen transversal cut along the plate has to be established.

The presented transformation from time to spatial coordinate arises from the last assumption in Coordinate system and simplifying assumptions (see page 3). We assume the presence of a precursor film of thickness equal to the intermediate region length scale, l, on the whole plate. Neglecting the long-range intermolecular forces, this precursor film can be taken as a free falling film. The point τ is then considered not to be directly on the three phase line, as there is, in fact none, but in the height l above the plate. Hence, τ is moving along x axis with the speed of

$$u_\tau = \frac{\rho g \sin\alpha}{2\mu} l^2. \tag{16}$$

Using this estimate for the speed of τ, the needed transformation is,

$$t = \varpi x, \qquad \varpi = \frac{2\mu}{\rho g \sin\alpha l^2}. \tag{17}$$

Substitution for t from (17) to (14) yields the equation defining the shape of the rivulet GL interface in the dependence on the plate longitudinal coordinate, x,

$$x - \frac{\bar{A}}{\beta^{15/4}}\left[\ln\left(\frac{B}{\beta^{3/4}}\right) - \frac{1}{5}\right] + \bar{C} = 0, \qquad \bar{A} = \frac{4}{15}\frac{A}{\varpi}, \quad \bar{C} = \frac{4}{15}\frac{C}{\varpi}. \tag{18}$$

With effects of the gravity If effects of the gravity on the shape of the rivulet GL interface cannot be neglected, specification of the interface shape becomes substantially more complicated. For the cases (i) and (iii), the equation (6) cannot be solved analytically and we cannot substitute for $a = a(\beta)$ in (11) as the relation is defined implicitly.

In the consequence, the equation (11) has to be solved numerically in the transformed coordinates $x = t/\varpi$. Moreover, the non-linear algebraic equation (6), defining the local contact angle $\beta = \beta(a(x))$, has to be solved in each iterator step.

Dimensionless coordinates and simulations All the variables except x were non-dimensionalized using the values at $x = 0$. For the non-dimensionalization of the plate longitudinal coordinate, x, the plate length, L, was used,

$$\xi = \frac{x}{L}, \quad \zeta = \frac{y}{a_0}, \quad \tilde{h} = \frac{h}{h_0^0}, \quad \tilde{\beta} = \frac{\beta}{\beta_0}, \tag{19}$$

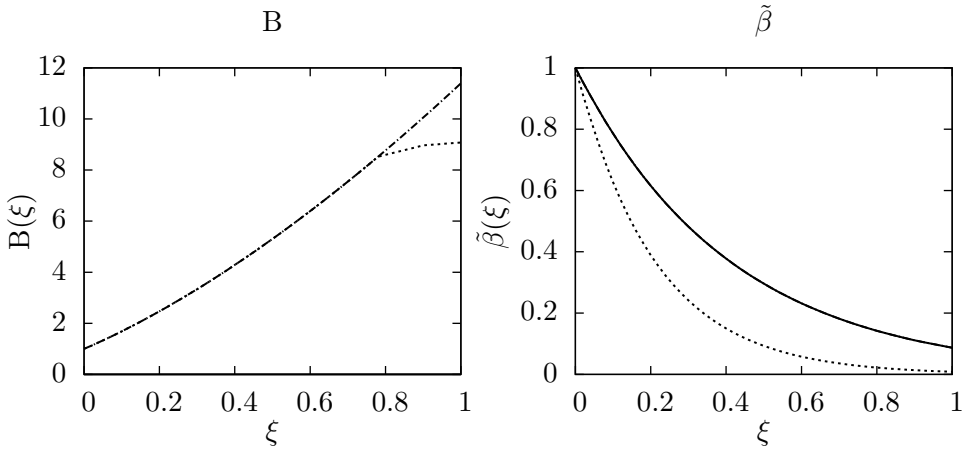

Figure 4: Change in the Bond number, B(ξ), and in the reduced dynamic contact angle, $\tilde{\beta}(\xi)$, along the rivulet. The three cases, (i) (-·-·-), (ii) (——) and (iii) (·····) are shown.

where a_0 and β_0 are the rivulet halw-width and dynamic contact angle at $\xi = 0$ tight together by the condition of a prescribed volume flux (6) and h_0^0 is the rivulet height at $\zeta = \xi = 0$. As the rivulet is spreading down the plate, $\tilde{\beta}(\xi)$ is decreasing and B(ξ) together with $\tilde{a}(\xi)$, are increasing as it is shown in the Fig. 4.

For the case of the plate inclination angle, α, greater than $\pi/2$, it can be seen, that the flow Bond number converges towards π^2 as the dynamic contact angle, $\tilde{\beta}$, vanishes. This corresponds to the fact, that for the case (iii), the GL interface is pulled from the plate by the gravity and

$$\lim_{\xi \to K \in \mathbb{R}^+} \tilde{\beta}(\xi) = 0, \tag{20}$$

meaning that at some finite distance, K, from the plate top, the surface tension and gravity forces reach an equilibrium and the spreading stops. This also follows directly from the analysis of the driving force for the spreading in the equation (11),

$$\frac{\mathrm{d}a(t)}{\mathrm{d}t} = 0 \iff \beta(t) = 0. \tag{21}$$

During the simulations, we considered a shallow water rivulet on a wetted substrate. The volume flux in the rivulet was fixed at $Q = 0.01\ \mathrm{ml\,s^{-1}}$,

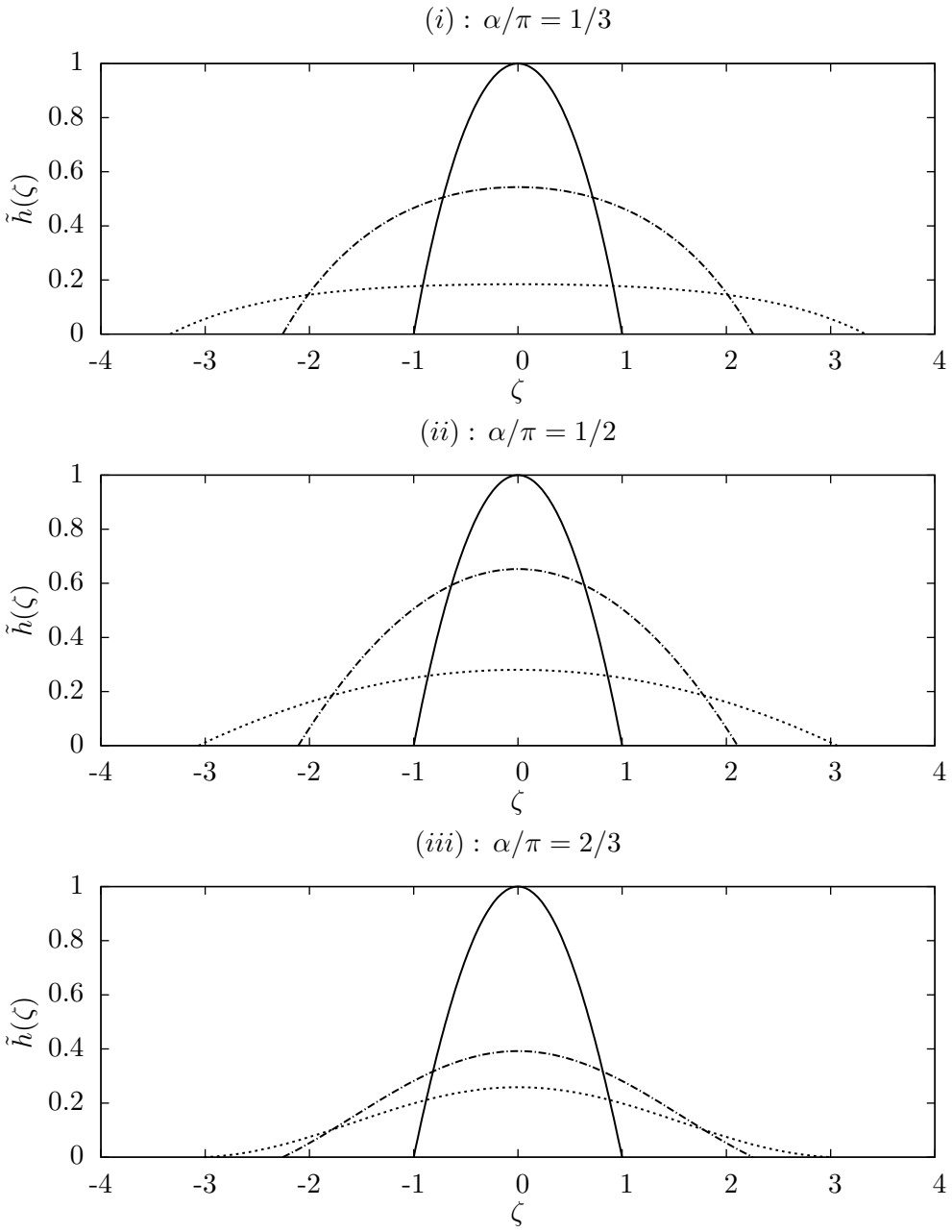

Figure 5: Evolution of the GL interface shape along the dimensionless plate longitudinal coordinate, ξ. Shapes of transversal cuts through the rivulet for the three cases are depicted at $\xi = 0$ (-·-·-), $\xi = 1/2$ (——) and $\xi = 1$ (·····).

the initial dynamic contact angle at $\beta_0 = 0.05 \ll 1$ and the rivulet initial half-width, a_0, was specified by the prescribed condition of $\mathrm{B} = 1$ at $x = 0$. The inclined plate length, L, was taken equal to 0.1 m.

The remaining parameter of the model: the intermediate region length scale, l, was fixed at $l = 3 \cdot 10^{-5}$ m. The selection of the value of l was based on our previous work, [25,26], and is in the agreement with literature on the topic (see [22,27] and references therein).

4 Velocity field

The velocity field in a steady rectilinear rivulet with unidirectional flow of a liquid is in a form of $\mathbf{u} = u(y, z)$. With the assumptions listed in Sec. 2, the velocity field can be derived analytically by solving the Navier-Stokes equations [6,11]. The obtained solution is in the form (consult the equation (5)),

$$u(\zeta, z) = \frac{\rho g \sin \alpha}{2\mu} \left(2h(\zeta) z - z^2 \right). \tag{22}$$

However, let us now consider a spreading but locally rectilinear rivulet. The velocity field of such a rivulet consists of all the three components, $\mathbf{u}(\mathbf{x}) = (u(\mathbf{x}), v(\mathbf{x}), w(\mathbf{x}))$.

The u component of the velocity field is approximately defined, at each discrete point of the solution of the ODE (11), by the relation (22). The contours of the u velocity component in the water rivulet spreading down a plate inclined by an angle $\alpha = \pi/3$ to the horizontal are depicted int the Fig. 6. Further informations on the selection of the simulation parameters can be found in the paragraph Dimensionless coordinates and simulations in the previous section. The u velocity field component was scaled using the velocity of the GL interface at the rivulet centerline, $\zeta = 0$, at the plate top, $\xi = 0$.

As for the v and w components of the velocity field, the presented method does not provide any approximate analytical solution. Thus, those two velocity components have to be simulated numerically. A technique similar to particle image velocimetry (PIV) was chosen.

PIV is an experimental technique which allows the velocity of fluid to be simultaneously measured throughout a region illuminated by a two-dimensional light sheet. Seeding particles are introduced into the flow and their motion is used to estimate the kinematics of the local fluid [24].

As the performed experiments were numerical, the seeding particles were defined artificially in a mesh-like manner. An algorithm for following the

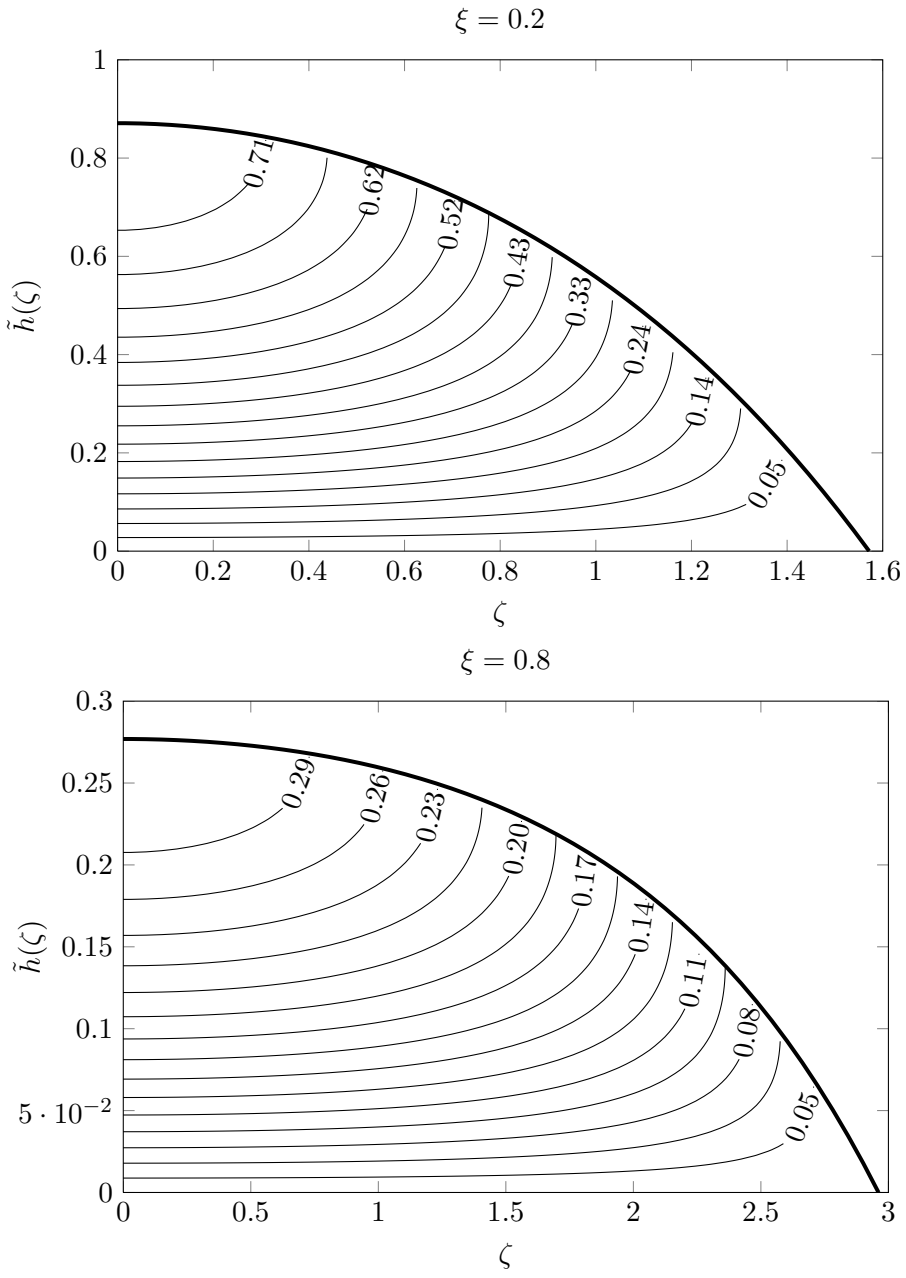

Figure 6: Contour plots of the $\tilde{u}$ component of the velocity field in a water rivulet flowing down a plate inclined by an angle $\alpha = \pi/3$ to the horizontal. For more details on the simulation see the paragraph Dimensionless coordinates and simulations in the previous section. The cases of $\xi = 0.2$ and $\xi = 0.8$ are shown.

evolution of the v and w velocity field components is described bellow. The whole proposed cycle has to be repeated for all N transversal cuts of the rivulet placed at $i\,\delta\xi$ from the plate top, where $i = 1, 2, \ldots, N$ and $\delta\xi$ is the time (distance) step prescribed by the solver used to treat the equation (11).

Velocity field tracking algorithm

- For each subrivulet do:
  1. Get the current width of the rivulet, ζ_i, from solution of the ODE (11).
  2. Calculate the current maximal rivulet height, $\tilde{h}_i^0$, from the equation (3).
  3. Create a mesh on a domain Ω_i,

$$\Omega_i = \left\{ (\zeta, \tilde{z}) \,:\, \zeta \in \langle 0; \zeta_i \rangle \mid \tilde{z} \leq \tilde{h}_i(\zeta) \right\}. \tag{23}$$

     The domain Ω_i represents a right half of the rivulet at a distance $i\,\delta\xi$ from the plate top. The left side of the rivulet can be neglected as the problem is axisymmetric along the x axis. The mesh itself is obtained by discretizing the domain Ω_i equidistantly in each coordinate by M_1 and M_2 points, respectively. The set of discrete points, Ω_i^h, is obtained,

$$\Omega_i^h = \left\{ (\zeta^j, \tilde{z}^k) \,:\, \zeta^j \in \langle 0; \zeta_i \rangle \;\middle|\; \tilde{z}^k \leq \tilde{h}_i(\zeta^j) \right\}_{j=1,\ldots,M_1;\, k=1,\ldots,M_2} \tag{24}$$

  4. Save the current mesh, Ω_i^h.
- Having saved all the local meshes, Ω_i^h, $i = 1, \ldots, N$, the velocity field in the $\zeta - \tilde{h}$ plane between individual transversal cuts can be calculated evaluating the change in the position of each mesh point along the rivulet.

In the Fig. 7, there are depicted the resulting velocity fields for the distances from the plate top $\xi = 0.2$ and $\xi = 0.8$ and the plate inclination angle $\alpha = \pi/3$. The slow down of the spreading can be observed as the contact angle, β, decreases.

Another interesting observation would be the fact, that the increase in the rivulet width is substantially quicker than the decrease in its height. This is due to the prescribed constant liquid flow rate and the parabolic velocity profile in the x axis direction.

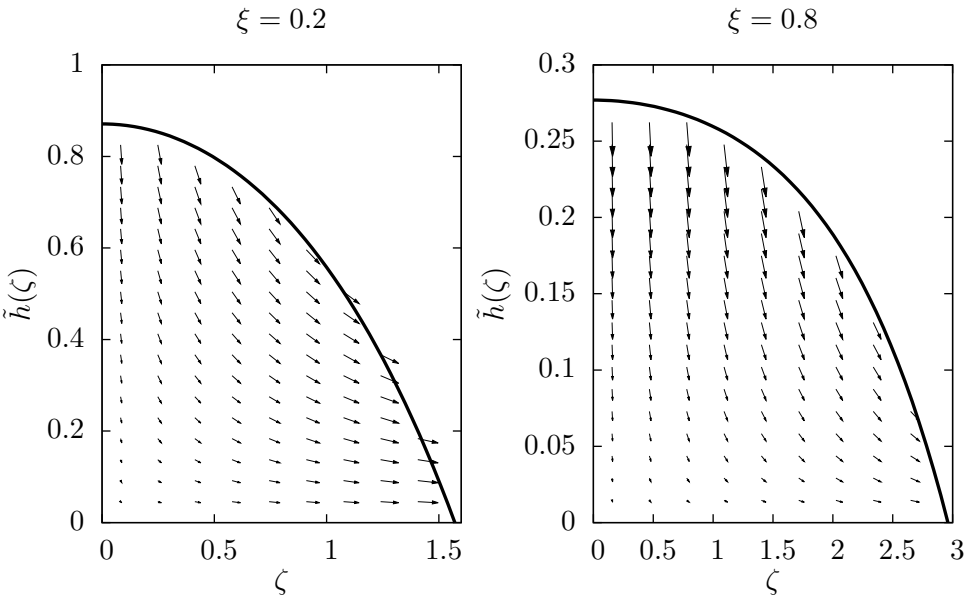

Figure 7: Comparison of the velocity fields in the $\zeta - \tilde{h}$ plane at $\xi = 0.2$ and $\xi = 0.8$. The case of a rivulet flowing down a plate inclined by $\alpha = \pi/3$ to the horizontal is depicted.

5 Conclusion

Even with the continuous growth of the computing capacity of modern computers, there is still a need for simplified solutions to the complex problems of fluid mechanics. Such method for the simulation of a rivulet spreading down an inclined wetted plate was derived and used to study the dependence of the liquid flow properties on various process parameters. Moreover, the derived model was used to describe the spreading itself and the evolution of the flow along an inclined plate without the necessity of solving the corresponding system of Navier-Stokes partial differential equations with a complex boundary condition describing the behaviour of the three phase line.

Nomenclature

a[m] ..... half-width of the rivulet
A, B, C, [s, −, −, −] ..... constants
B[−] ..... Bond number
e[−] ..... Euler's constant
g[m s^{-2}] .. gravitational acceleration
h[m] ..... height

l[m] intermediate region length scale
L[m] ..... total rivulet length
M_1, M_2[−] ...number of meshpoints
N[−] ...number of consecutive cuts
p[Pa] ..... pressure
Q[m^3 s^{-1}] .....volumetric flow rate
S[m^2] ..... size of the interface
t[s] ..... time coordinate
(u, v, w)[m s^{-1}] .....velocity field
x, y, z[m] ..... coordinate system

Greek letters

α[−] ..... plate inclination angle
β[−] ..... dynamic contact angle
γ[N m^{-1}] .....liquid surface tension
δ[−] .....small difference
$\eta[m]$ .....constant defined in the equation (10)
ζ, ξ[−] ..... dimensionless x, y coordinates
μ[Pa s] .....liquid dynamic viscosity
ϖ[m^{-1} s] transformation from t to x
ρ[kg m^{-3}] ..... liquid density
τ[−] . contact point for 2D interface
Ω[−] ..... domain of the rivulet transversal cut

References

[1] J. J. Cooke, S. Gu, L. M. Armstrong, K. H. Luo, *Gas-liqud flow on smooth and textured inclined planes*, World Ac. of Sc., Eng. and Technol., Vol.68. (2012), pp.1712-1719.

[2] R. Maiti, R. Khanna, K.D.P. Nigam, *Hysteresis in trickle-bed reactors: a review*, Ind. Eng. Chem. Res., Vol.45. (2006), pp.5185-5198.

[3] P. Vlasogiannis, G. Karagiannis, P. Argyropoulos, V. Bontozoglou, *Airwater two-phase flow and heat transfer in a plate heat exchanger*, Int. J. Multiph Flow, Vol.25. (2002), pp.757-772.

[4] S.F. Kistler, P.M. Schweizer (Eds.). *Liquid Film Coating*, Chapman and Hall, London, (1997)

[5] A. Ataki, P. Kolb, U. Bühlman, H. J. Bart, *Wetting performance and pressure drop of structured packing: CFD and experiment*, I. Chem. E. – symp. series, Vol.152. (2009), pp.534-543.

[6] G.D. Towell, L.B. Rothfeld, *Hydrodynamics of rivulet flow*, A. I. Ch. E. J., Vol.12. (1966), pp.972-980.

[7] R.F. Allen, C.M. Biggin, *Longitudinal flow of a lenticular liquid filament down an inclined plane*, Phys. Fluids, Vol.17. (1974), pp.287-291.

[8] M. Bentwich, D. Glasser, J. Kern, D. Williams, *Analysis of rectilinear rivulet flow*, A. I. Ch. E. J., Vol.22. (1976), pp.772-779.

[9] I. M. Fedotkin, G. A. Melnichuk, F. F. Koval, E. V. Klimkin, *Hydrodynamics of rivulet flow on a vertical surface*, Inz.-Fiz. Zhurnal, Vol.46, No.1. (1984), pp.14-20.

[10] E.S. Benilov, *On the stability of shallow rivulets*, J. Fluid Mech., Vol.636. (2009), pp.455-474.

[11] B.R. Duffy, H.K. Moffatt, *Flow of a viscous trickle on a slowly varying incline* Chem. Eng. J., Vol.60 (1995), pp.141-146.

[12] P.A. Kuibin, *An asymptotic description of the rivulet flow along an inclined cylinder*, Russ. J. Eng. Thermophys., Vol.6. (1996), pp.33-45.

[13] C. A. Perazzo, J. Gratton, *Navier-Stokes solutions for parallel flow in rivulets on an inclined plane*, J. Fluid Mech., Vol.507. (2004), pp.367-379.

[14] S. K. Wilson, J. M. Sullivan, B. R. Duffy, *The energetics of the breakup of a sheet and of a rivulet on a vertical substrate in the presence of a uniform surface shear stress*, J. Fluid Mech., Vol.674. (2011), pp.281-306.

[15] C. Paterson, S. K. Wilson, B. R. Duffy, *Pinning, de-pinning and re-pinning of a slowly varying rivulet*, Eur. J. Mech. B/Fluids, Vol.41. (2013), pp.94-108.

[16] S.H. Davis, *Moving contact lines and rivulet instabilities, Part 1. The static rivulet*, J. Fluid Mech., Vol.90. (1980), pp.225-242.

[17] S. A. Shetty, R. L. Cerro *Spreading of liquid point sources over inclined solid surfaces* Ind. Eng. Chem. Res., Vol.34. (1995), pp. 4078-4086.

[18] M. Renardy, Y. Renardy, J. Li, *Numerical simulation of moving contact line problems using a volume-of-fluid method*, J. Comp. Phys., Vol.171. (2001), pp.243-263.

[19] K. V. Meredith, A. Heather, J. De Vries, Y. Xin, *A numerical model for partially-wetted flow of thin liquid films*, Comp. Meth. Multiph. Flow, Vol.70. (2011), pp.239-250.

[20] J. A. Diez, A. G. Gonzáles, L. Kondic, *On the breakup of fluid rivulets*, Phys. Fluids, Vol.21. (2009), pp.1-15.

[21] O. V. Voinov, *Hydrodynamics of wetting*, Fluid Dyn., Vol.11. (1976), pp.714-721 (English translation).

[22] R. G. Cox, *Thedynamics of spreading of liquids on a solid surface. Part 1. Viscous flow*, J. Fluid Mech., Vol.168 (1986), pp.169-194.

[23] D. Bonn, J. Eggers, J. Indekeu, J. Meunier, E. Rolley, *Wetting and spreading*, Rev. Mod. Phys., Vol.81. (2009), pp.739-805.

[24] I. Grant, *Particle image velocimetry: a review*, Proc. Inst. Mech. Engrs., Vol.211. (1997), pp.55-76.

[25] M. Isoz, *Study of the rivulet type flow of a liquid on an inclined plate*, Master thesis, ICT Prague, 2013

[26] M. Isoz, *Computationally inexpensive method to determine size of gas-liquid interfacial area of rivulet spreading in inclined wetted plate*, Proceeding of conference *Topical problems of fluid mechanics 2014*, Prague (2014), pp.59-62.

[27] S. Middleman, *Modeling axisymmetric flows*, Academic Press, London, 1995

Acknowledgments: The presented work was supported by IGA of ICT Prague, under the grant number A2_FCHI_2014_001.